

High p_T : Electroweak and QCD results from ATLAS

Alejandro Alonso on behalf of the ATLAS Collaboration
University of Lund, Post Box 117, 22446 Lund, Sweden

DOI: <http://dx.doi.org/10.5689/UA-PROC-2010-09/02>

By August 2010 the ATLAS detector had collected more than 3 nb^{-1} of proton-proton collision data at $\sqrt{s} = 7 \text{ TeV}$. The latest results on high transverse momentum physics are presented. For electroweak measurements, cross sections for Z and W boson production in leptonic channels are presented, and the lepton charge asymmetry arising from differences between W^+ and W^- boson production is shown. With regards to QCD, the differential inclusive jet cross section is measured, and the dependence on invariant mass of the di-jets cross-section is shown. Another important QCD channel for early measurements is top quark production. Latest candidate events are shown. The last topic to be shown in this paper is direct photon production.

1 Introduction

The ATLAS detector [1] is a large multi-purpose detector operating at the CERN Large Hadron Collider (LHC). It has been designed to study multiple physics processes. The very first benchmark for the ATLAS experiment is to achieve a complete and detailed understanding of known physics, in particular the Standard Model processes. During the first months of proton-proton collisions at $\sqrt{s} = 7 \text{ TeV}$, in addition to much effort on commissioning, many physics analyses have been performed.

In this paper we introduce some selected results for high transverse momentum processes in Electroweak and QCD physics. A good understanding of high transverse momentum processes is fundamental to understanding our detector, checking the predictions of the Standard Model and getting ready for discovery in models beyond it. For electroweak measurements, we start by presenting the Z and W bosons cross sections in the electron and muon channels, together with the Z invariant mass. Also, the asymmetry in W^+ and W^- production is shown. Understanding QCD at 7 TeV is an important challenge itself and for background estimations for other processes, so we show the cross section measured for single and di-jet production. In top physics, with the analyzed luminosity, few events have been seen and we briefly describe them. The last topic presented is the evidence of direct photon production.

2 Electroweak Measurements

The experimental study of the electroweak gauge bosons has a history of about thirty years. W and Z bosons decaying to electrons and muons are the first physics signatures with high

transverse momentum leptons observed in ATLAS. The well-known properties of the Z boson provide significant constraints in the determination of the performance of the collider experiments at the LHC; its known mass, width and leptonic decays can be exploited to determine the detector energy and momentum scale and resolution, as well as lepton identification and trigger efficiencies.

In Figure 1 the invariant mass of the $Z/\gamma^* \rightarrow ll$ candidates [2] for electron and muon channels is presented using an accumulated luminosity of 914 nb^{-1} and 1.07 pb^{-1} respectively. The data are modelled using the theoretical line shape, including photon and Z contributions, convolved with a gaussian resolution function. The fitted peak of the distribution is found to be $90.9 \pm 0.3 \text{ GeV}$ in the electron channel and $90.8 \pm 0.3 \text{ GeV}$ in the muon channel (with values of 91.6 GeV and 91.3 GeV , respectively, from the Monte Carlo). The experimental resolutions are found to be $3.2 \pm 0.3 \text{ GeV}$ and $3.3 \pm 0.3 \text{ GeV}$ (with values of 1.8 GeV and 1.5 GeV from the Monte Carlo), respectively.

In addition to performance studies, ATLAS will analyze W and Z boson production at a previously unexplored energy scale. These will provide new insights on the proton properties constraining its parton density functions, tests of perturbative QCD calculations, and ultimately a precise determination of the mass of the W boson. In Figure 2 the first measured values of the production cross sections [2, 3] in the electron and muon channels for Z and W bosons for accumulated luminosity of 225 nb^{-1} and 17 nb^{-1} respectively are shown. The results obtained are in agreement with the theoretical calculations based on NNLO QCD using the FEWZ program [4] with the MSTW2008 set of parton distribution functions [5].

The measurement of the excess of W^+ over W^- in proton proton collisions provides important information about parton density functions (PDFs), particularly the difference between u and d valence quark contributions. The asymmetry is measured as:

$$A = \frac{\sigma^{l^+} - \sigma^{l^-}}{\sigma^{l^+} + \sigma^{l^-}} \quad (1)$$

where σ^l are the fiducial cross sections, i.e. cross sections used are not corrected for the geometrical acceptance and kinematic selection. Figure 3 shows the asymmetry in two regions of lepton pseudo-rapidity. The measurements are in agreement with the theoretical predictions obtained with NLO calculations, namely MC@NLO [6] and DYNLO [7] which have been interfaced to various PDF parameterizations of the respective order. The parton distribution functions MSTW08 [5], CTEQ6.6 [8] and HERAPDF1.0 [9] were used.

3 Jet physics

At the LHC, jet production is the dominant high transverse momentum process and as such gives us a glimpse of physics at the TeV scale. Jet rates and cross sections are key observables in high-energy particle physics. They provide precise measurements of the strong coupling constant. They can be used to obtain information about the structure of the proton. Furthermore they have become an important tool for understanding the strong interaction and searching for physics beyond the Standard Model. The inclusive jet and di-jet cross sections have been measured [10] using 17 nb^{-1} of data. Jets are reconstructed from calorimeter clusters using the anti- k_T algorithm, which is infrared and collinear safe, with a resolution parameter R of 0.4 or 0.6. The data were compared to NLO perturbative QCD calculations based on NLOJET++ 4.1.2 [11] where CTEQ 6.6 [8] NLO parton densities were used. In addition predictions were

corrected for non-perturbative effects. Figure 4(a) shows the single-jet cross section as a function of jet transverse momentum with $R=0.6$ and Figure 4(b) shows the di-jet cross section as a function of di-jet mass with $R=0.6$. In both cases the data are shown for different rapidity ($|y|$) bins. The measured regions for jet cross sections extend up to jet p_T of 500 GeV and di-jet masses of 2 TeV. The dominant systematic uncertainty is due to the jet energy scale [12], which is below 9% over the entire range of p_T and y and below 7% for central jets with $p_T > 60$ GeV. Particle-level predictions based on NLO perturbative QCD are in good agreement with the observed cross sections.

4 Top physics

The re-discovery of top quark pair production is one of the key milestones for the early LHC physics program. A search for candidate events consistent with top quark pairs decaying into lepton plus jets and di-lepton plus jets has been made using 280 nb^{-1} of data at $\sqrt{s}=7 \text{ TeV}$ [13]. Nine candidate events were observed; 7 lepton-jet candidates and 2 di-lepton plus jet candidates. In Figure 5 the invariant mass of the 3-jet combination having the highest p_T for the four events selected in electron plus jets and the three events in muon plus jets channels are presented. The kinematic properties of the nine events selected are consistent with top quark pair production. A larger data sample and further study of control regions are required before a conclusive statement on the observation of top quark production in ATLAS can be made. The lepton plus jets channel suffers from significant background contributions from other Standard Model processes so a detailed study of the background in this channel has been done [14] with an integrated luminosity of 295 nb^{-1} . This analysis shows that the measurement of top background is in agreement with the expectations at this early stage.

5 Direct Photon Production

In the Standard Model, the cross section for inclusive prompt photon production at LHC energies is expected to be large, $O(\mu\text{b})$, for transverse energies above 10 GeV. Prompt photon production at hadron colliders provides a handle for testing perturbative QCD predictions. It can also be used to constrain parton structure functions and is important for many physics signatures, including searches for the Higgs boson. A search of this process [15] has been performed in ATLAS with a modest integrated luminosity of 15.8 nb^{-1} . In this analysis a data-driven method is used to estimate the background and extract the prompt photon signal. In Figure 6 the purity of the photon sample can be seen. For transverse energy above 20 GeV a signal yield of (618 ± 75) prompt photons with a purity of $(72 \pm 7)\%$ is measured. Together with the first estimates of the photon efficiency measurement, this gives confidence that a measurement of the prompt photon production cross section will be soon possible and physics studies with photons in the final states are promising.

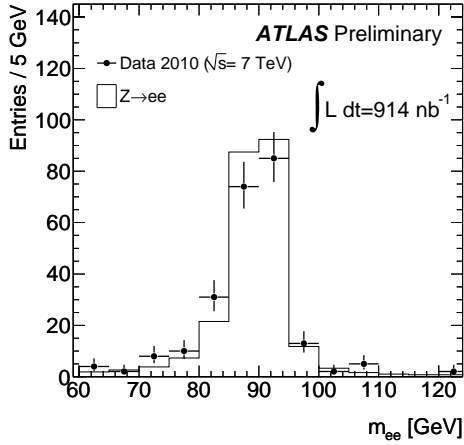
6 Summary

LHC operation at 7 TeV has started, and the ATLAS experiment is fully operational. It is just starting to explore its vast collision physics program, Standard Model physics being the first benchmark. In this paper a brief review of the latest high momentum physics has been

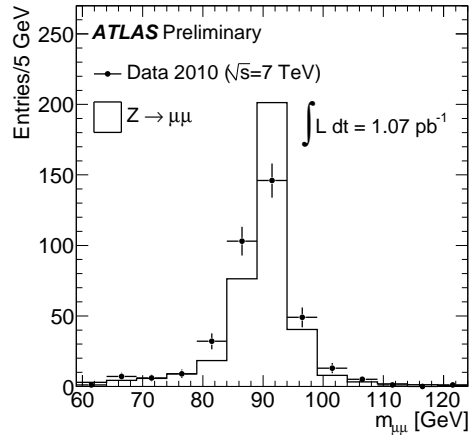
presented. The first measurements of W and Z boson production cross sections have been presented showing a good agreement with the theoretical predictions at NNLO. For QCD, the inclusive cross section for single-jet and di-jet production has been shown and compared the NLO prediction, showing a very good agreement. From this study, it is clear from the early data that the jet performance in the ATLAS detector is well understood. Nine events consistent with the top quark production have been found in the lepton+jet and di-lepton+jets channels. The last measurement presented is the prompt photon production. For transverse energies above 20 GeV prompt photons are measured with a purity of $(72 \pm 7)\%$. All these analyses, in addition to new ones, will be updated with higher accumulated luminosity. The smaller statistical errors, together with improved detector understanding, will allow more precise measurements of the Standard Model processes in the future.

References

- [1] ATLAS Collaboration, JINST **3**, S08003 (2008).
- [2] ATLAS Collaboration, ATLAS-CONF-2010-076 [<http://cdsweb.cern.ch/record/1281367>].
- [3] ATLAS Collaboration, ATLAS-CONF-2010-051 [<http://cdsweb.cern.ch/record/1281306>].
- [4] C. Anastasiou, L. J. Dixon, K. Melnikov and F. Petriello, Phys. Rev. D **69**, 094008 (2004) [arXiv:hep-ph/0312266].
- [5] A. D. Martin, W. J. Stirling, R. S. Thorne and G. Watt, Eur. Phys. J. C **63** (2009) 189 [arXiv:0901.0002 [hep-ph]].
- [6] S. Frixione and B. R. Webber, JHEP **0206**, 029 (2002) [arXiv:hep-ph/0204244].
- [7] S. Catani and M. Grazzini, Phys. Rev. Lett. **98**, 222002 (2007) [arXiv:hep-ph/0703012].
- [8] P. M. Nadolsky *et al.*, Phys. Rev. D **78**, 013004 (2008) [arXiv:0802.0007 [hep-ph]].
- [9] F. D. Aaron *et al.* [H1 and ZEUS Collaboration], JHEP **1001**, 109 (2010) [arXiv:0911.0884 [hep-ex]].
- [10] ATLAS Collaboration, ATLAS-CONF-2010-050 [<http://cdsweb.cern.ch/record/1281305>].
- [11] Z. Nagy, Phys. Rev. D **68**, 094002 (2003) [arXiv:hep-ph/0307268].
- [12] ATLAS Collaboration, ATLAS-CONF-2010-056 [<http://cdsweb.cern.ch/record/1281329>].
- [13] ATLAS Collaboration, ATLAS-CONF-2010-063 [<http://cdsweb.cern.ch/record/1281338>].
- [14] ATLAS Collaboration, ATLAS-CONF-2010-087 [<http://cdsweb.cern.ch/record/1298967>].
- [15] ATLAS Collaboration, ATLAS-CONF-2010-077 [<http://cdsweb.cern.ch/record/1281368>].

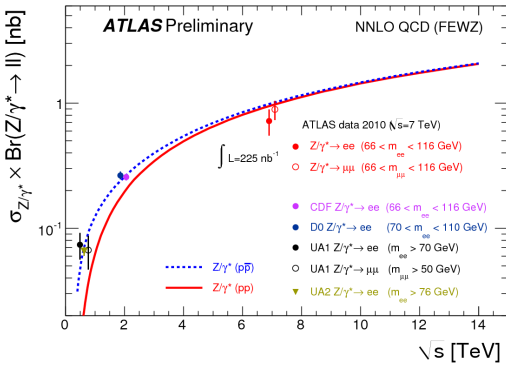


(a)

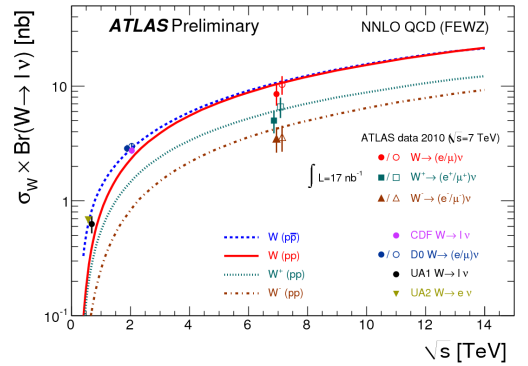


(b)

Figure 1: Distributions of the invariant mass $m_{\ell\ell}$ of Z candidates in the electron 1(a) and muon 1(b) channels. The data are compared to the expectations from Monte-Carlo simulation.

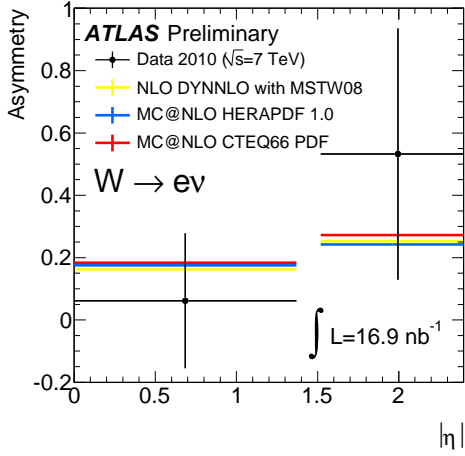


(a)

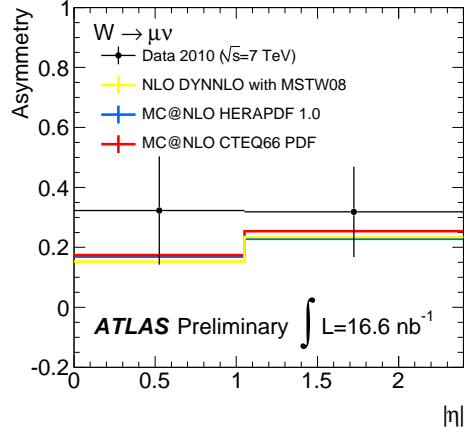


(b)

Figure 2: 2(a) The measured value of $\sigma_Z \times BR(Z \rightarrow l\bar{l})$ for the electron and muon channels. 2(b) The measured value of $\sigma_W \times BR(W \rightarrow l\nu)$ for W^+ , W^- for the electron and muon channels. The data are compared to theoretical predictions based on NNLO calculations for both proton proton and proton anti-proton collisions as a function of the centre-of-mass energy \sqrt{s} . Measurements from previous proton anti-proton colliders are also shown.

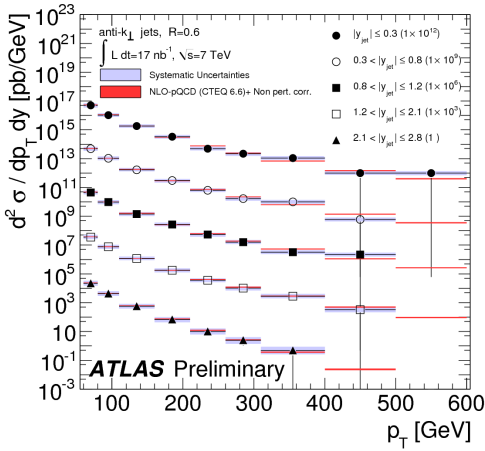


(a)

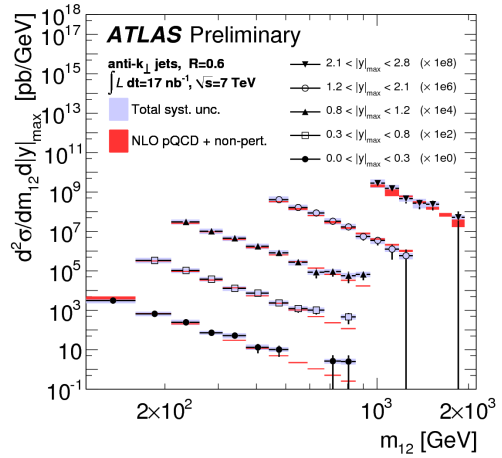


(b)

Figure 3: W charge asymmetry in the electron channel 3(a) and muon channel 3(b) as a function of the lepton pseudo-rapidity compared to various theoretical predictions.



(a)



(b)

Figure 4: 4(a) Inclusive jet differential cross section as a function of jet p_T in different regions of rapidity for jets identified using the anti- k_T algorithm with $R=0.6$. 4(b) Di-jet differential cross section as a function of di-jet mass, binned in the maximum rapidity of the 2 leading jets. The errors bars indicate the statistical uncertainty on the measurement and the grey shaded band indicates the quadratic sum of the systematic uncertainties. An additional 11% uncertainty due to the luminosity measurement is not shown. The theory uncertainty is shown in red.

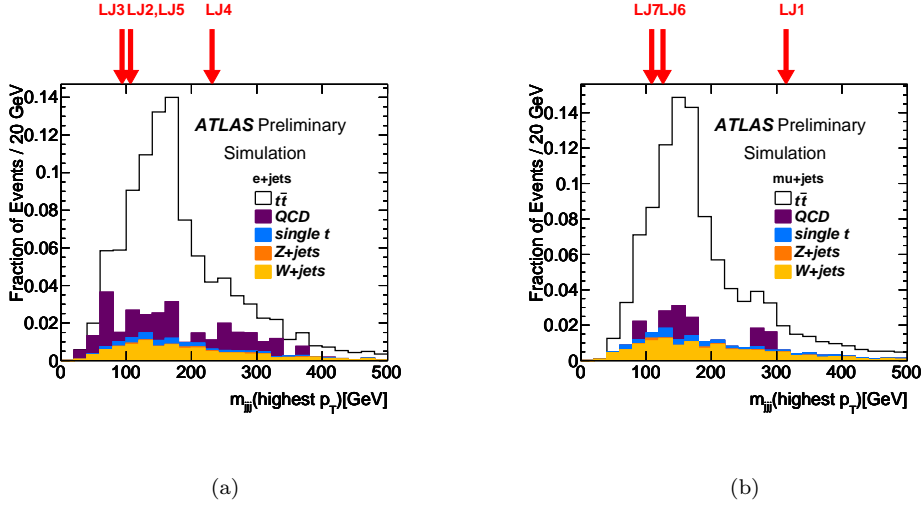


Figure 5: Distribution of m_{jjj} , the invariant mass of the 3-jet combination having the highest p_T , for events passing the electron plus jets selection 5(a) and passing the muon plus jets selection 5(b). In both figures the positions of data candidate events are indicated by arrows.

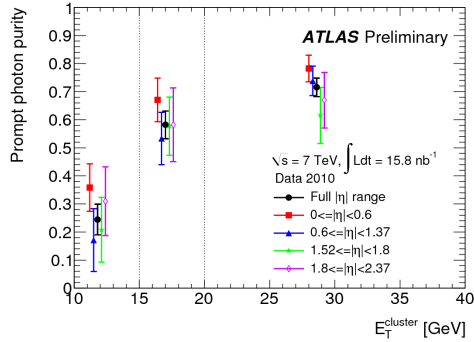


Figure 6: Estimated prompt photon purity in data, as a function of photon transverse energy, for four different pseudo-rapidity bins and in the whole $|\eta|$ range ($|\eta| \leq 2.37$). The points corresponding to the measurements in whole $|\eta|$ range (full circles) have been positioned, along the horizontal axis, at the average transverse energy of all selected photon candidates in the signal region in data, in the three intervals: $10 \leq E_T < 15$ GeV, $15 \leq E_T < 20$ GeV and $E_T \geq 20$ GeV (identified by the dotted vertical lines). The points corresponding to the measurements in subintervals of the full $|\eta|$ range have been displaced arbitrarily along the horizontal axis.